Enhancing tumor-infiltrating T cells with an exclusive fuel source

Matthew L. Miller 1,2, Rina Nagarajan 3, Timothy J. Thauland 3, Manish J. Butte 1,2,3,4,*

Affiliations

1. Molecular Biology Institute, UCLA; Los Angeles, CA, USA.
2. Department of Microbiology, Immunology, and Molecular Genetics, UCLA; Los Angeles, CA, USA.
3. Division of Immunology, Allergy, and Rheumatology; Department of Pediatrics, UCLA; Los Angeles, CA, USA.
4. Department of Human Genetics, UCLA; Los Angeles, CA, USA.

* Corresponding author. Email: mbutte@mednet.ucla.edu

Summary

Solid tumors harbor immunosuppressive microenvironments that inhibit tumor infiltrating lymphocytes (TILs) through the voracious consumption of glucose. We sought to restore TIL function by providing them with an exclusive fuel source. The glucose disaccharide cellobiose, which is a building block of cellulose, contains a β-1,4-glycosidic bond that cannot be hydrolyzed by animals (or their tumors), but fungal and bacterial organisms have evolved enzymes to catabolize cellobiose and use the resulting glucose. By equipping T cells with two proteins that enable import and hydrolysis of cellobiose, we demonstrate that supplementation of cellobiose during glucose withdrawal restores T cell cytokine production and cellular proliferation. Murine tumor growth is suppressed and survival is prolonged. Offering exclusive access to a natural disaccharide is a new tool that augments cancer immunotherapies. Beyond cancer, this approach could be used to answer questions about the regulation of glucose metabolism across many cell types, biological processes, and diseases.

Introduction

Glucose is a critical fuel for cellular bioenergetics and a major source of biosynthetic precursors for anabolic pathways. Upon antigen stimulation, CD8+ T cells extensively rewire their metabolism and robustly engage aerobic glycolysis to support the various functions required of cytotoxic T cells, including survival, proliferation, cytokine production, and cytotoxicity. Abnormally low glucose concentrations are found in the tumor microenvironment (TME) of solid tumors due to the voracious nature of tumor metabolism, leading to a competition for glucose that contributes to cancer progression[1–8] due to stunted T-cell effector functions[9–12]. We hypothesized that TILs provisioned with an *exclusive* source of glucose that was inaccessible to cancer cells would be invigorated, allowing them to fulfill their role in clearing tumors more effectively.

Cellobiose, a glucose disaccharide that comprises cellulose and is found abundantly in plant matter, has great potential to serve as a carbon and energy source but remains inert to catabolic processes in animal cells for two primary reasons. First, metazoan sugar transport is restricted to monosaccharides. Second, the β-1,4-glycosidic bond that joins glucose molecules in cellobiose cannot be efficiently hydrolyzed by metazoan glycoside hydrolases[13,14]. The transport and hydrolyzation of cellobiose, on the other hand, can be efficiently carried out in cellulolytic microbes such as fungi and bacteria[15–17]. Thus, cellobiose could offer an exclusive source of glucose for engineered T cells, as it is inaccessible to tumors.

Here, we report that the heterologous expression of a cellobiose transporter and a β-glucosidase from the mold *Nuerospora crassa* in primary T cells endows them with the ability to robustly catabolize cellobiose, which rescues T cells from glucose deprivation. We demonstrate that tumor cells lack the ability to use cellobiose, allowing this nutrient to exclusively support the metabolism of T cells. Finally, we show that enabling engineered T cells to overcome the glucose restriction of the tumor microenvironment allows for an increased capacity to clear tumors.

Results

Heterologous and Functional Expression of Cellobiose Catabolism Proteins in Primary T cells

To impart the ability to catabolize cellobiose as a fuel source for glycolysis, only two proteins are needed: 1) a transporter of cellobiose from the extracellular to intracellular space; and 2) a β-glucosidase that can efficiently hydrolyze the β-1,4 bond that joins the glucose molecules in cellobiose. We chose to work with a pair of previously characterized proteins from *Neurospora crassa*, namely, the cellobiose transporter CDT-1 and the cellobiose glucosidase GH1-1 (**Fig. 1a**), which were reported to enable cellobiose catabolism through heterologous expression into yeast[18].

We optimized the codon sequence of each gene for murine expression (**Fig. S1**) and cloned them into mouse stem cell viral vectors (**Fig. 1b**). Each transgene was appended with a hemagglutinin (HA) tag and coupled to a discrete fluorescent protein via a 2A peptide sequence. Staining of transduced, primary CD8+ T cells for the HA tag revealed robust expression of both of the genes, which was demonstrated to be coupled to their fluorescent reporters (**Fig. 1c**). To confirm the subcellular localization of each protein, we immunostained T cells and performed confocal microscopy. CDT-1 localizes to the periphery of the T cell, which is consistent with its function as a transporter. In contrast, the distribution of GH1-1 is more diffuse, indicative of a cytosolic localization and consistent with the localization of other enzymes involved in the glycolytic pathway[19] (**Fig. 1d**).

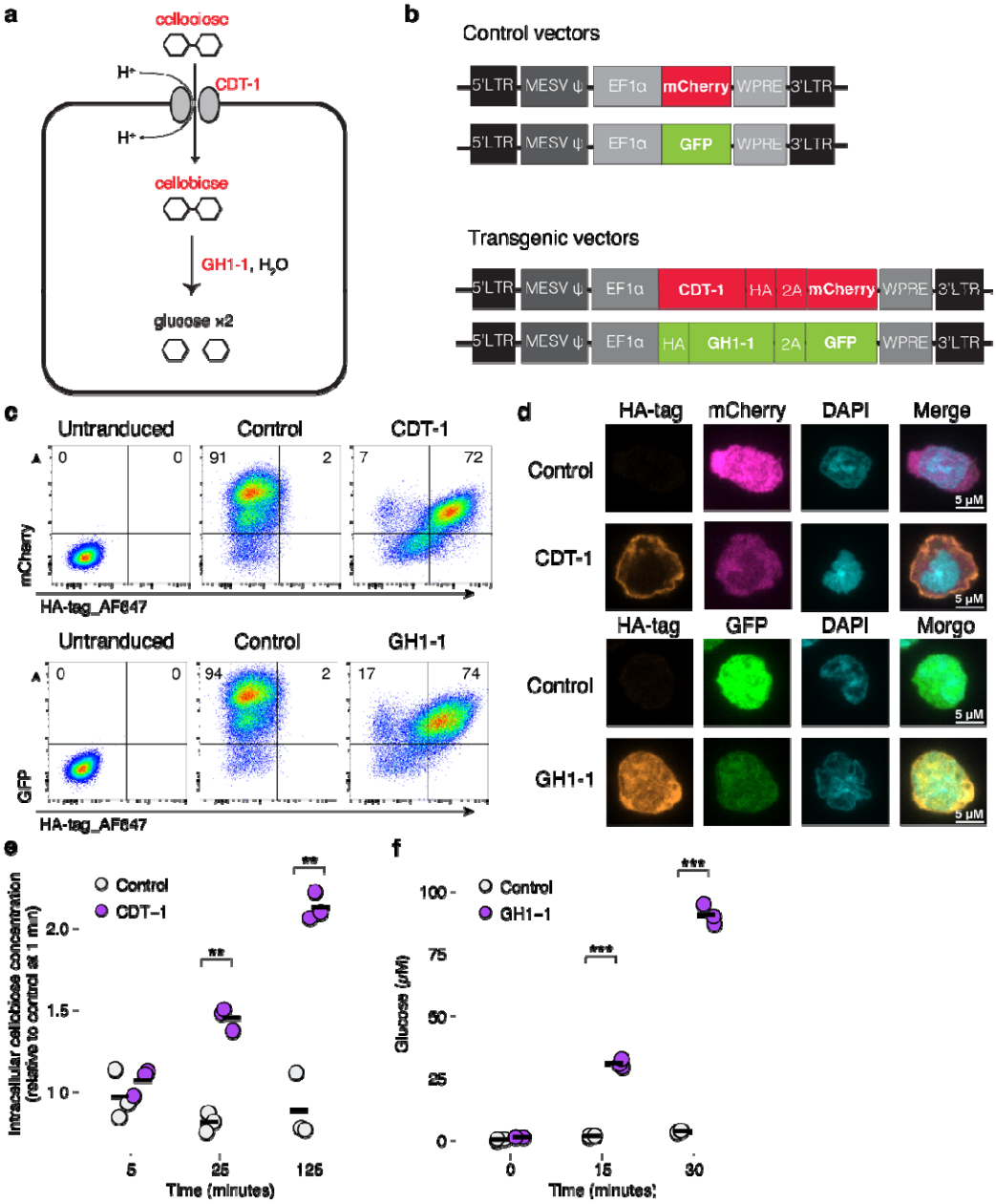

Fig. 1. Heterologous expression of two proteins from fungi allow for cellobiose import and hydrolysis in T cells. **a)** Schematic of cellobiose transport through the proton symporter CDT-1, followed by hydrolysis by the cellobiose glucosidase GH1-1. Once glucose is liberated within the cell it may flow through the standard glycolytic pathway. **b)** Schematic of mouse stem viral vectors. Control vectors express fluorescent protein alone and transgenic vectors couple transgenic expression to fluorescent protein expression with a 2A peptide motif. Expression is driven by a constitutive EF1a promoter and enhanced with a woodchuck hepatitis virus post-transcriptional regulatory element (WPRE). **c)** Transgene and fluorescent protein expression analysis in transduced, primary, mouse T cells. **d)** Confocal microscopy images showing localization of CDT-1 (top) and GH1-1 (bottom), fluorescent proteins, and nuclei (DAPI) in transduced, primary, mouse T cells. **e)** CDT-1 transport assay. Control and CDT-1 transduced mouse T cells were incubated with 5 mM cellobiose before extracting intracellular metabolites for LC-

MS quantification. **f)** GH1-1 hydrolysis assay. Control and GH1-1 transduced mouse T-cell lysates were incubated with 1 mM cellobiose before quantification of glucose with an Amplex Red glucose assay kit (Thermo). Horizontal lines indicate means. Statistical significance was assessed using an unpaired t-test in E and F (*p□<□0.05; **p□<□0.01; ***p□<□0.001; NS□>□0.05). Data shown in **e** and **f** are means of technical replicates (n=3) from one experiment and are representative of at least two independent experiments.

We next sought to confirm the functionality of each transgenic protein. To test the capacity of CDT-1 to transport cellobiose, we incubated transduced T cells with cellobiose, extracted intracellular metabolites, and performed liquid chromatography-mass spectrometry (LC-MS). We found that cellobiose accumulated in the intracellular metabolite pool at a higher rate in T cells expressing CDT-1 compared to control cells (**Fig. 1e**). To evaluate the functionality of GH1-1 as a cellobiose glucosidase, we transduced T cells with GH1-1, generated cellular lysates, incubated with cellobiose, and quantified the resultant glucose yield. We found that GH1-1 expression significantly increased the glucose concentration over time (Fig. 1f). Taken together, we have developed a system wherein primary T cells co-transduced with the genes CDT-1 and GH1-1 (referred to as CG-T cells) are endowed with the necessary machinery to utilize extracellular cellobiose as a source of intracellular glucose.

Transgenic T cells Robustly Catabolize Cellobiose to Fuel Glycolysis

To test if CG-T cells are capable of catabolizing cellobiose, we incubated control and CG-T cells with copious, isotopically labelled U-$^{13}C_{12}$ cellobiose in the presence of a low concentration of unlabeled glucose (**Fig. 2a**). We observed extensive carbon labeling in key metabolites of the glycolytic, pentose phosphate, and tricarboxylic (TCA) pathways in CG-T cells (**Fig. 2b**), with cellobiose contributing nearly 100% of the carbons present in glycolytic metabolites such as fructose 1,6-bisphosphate, 3-phosphoglyceric acid, and phosphoenolpyruvate. In stark contrast, control cells showed negligible labeling of intracellular metabolites, an expected result that confirms our conventional understanding that mammalian cells lack the capacity to metabolize cellobiose.

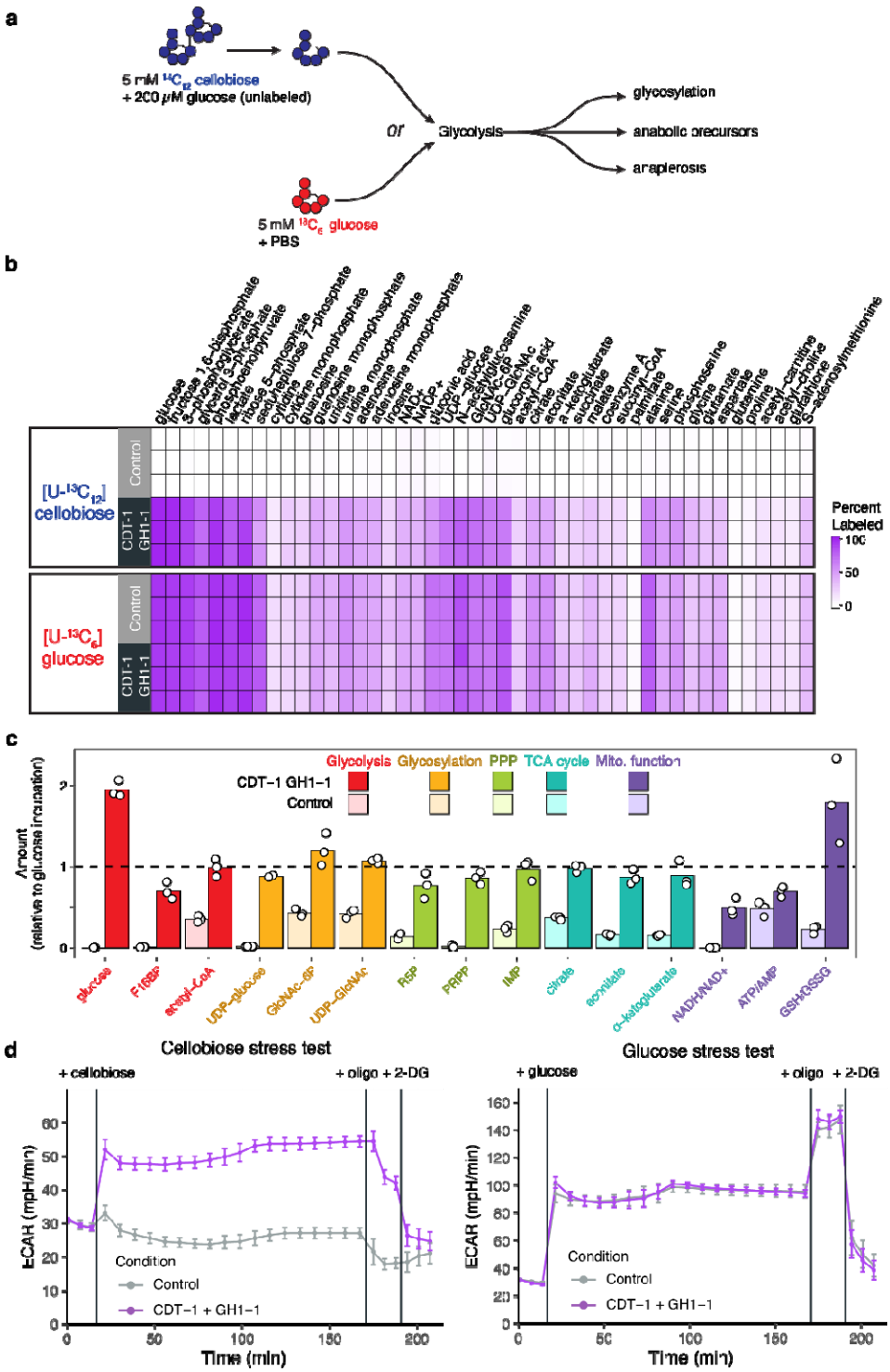

Fig. 2. Transgenic T cells metabolize cellobiose and replenish metabolic pathways during glucose withdrawal. a) Schematic of isotopically labeled sugar experiment. Transduced T cells were incubated with either 5 mM universally 13C-labeled cellobiose and 200 μM unlabeled glucose or 5 mM universally 13C-labeled glucose for 16 h before intracellular metabolites were extracted for analysis by LC-MS. **b**) Heat map displaying the percent labeling of intracellular metabolites from transduced T cells incubated with isotopically labeled cellobiose or isotopically labeled glucose. **c**) Abundance of intracellular metabolites during cellobiose

incubation relative to their abundance during glucose incubation. PPP, pentose phosphate pathway. **d**) Cellobiose and glucose stress tests using a XFe96 Seahorse Flux Analyzer. Transduced T cells had basal measurements taken before injection of cellobiose or glucose from the first port. Oligomycin A was injected from the second port and 2-deoxyglucose (2-DG) injected from the third port. ECAR, extracellular acidification rate. Error bars represent standard deviation of the mean, n=12. Data shown in b and c are from technical replicates (n=3) of one experiment and are representative of at least two independent experiments.

To determine whether cellobiose carbons are fluxing through the standard glycolytic pathway, we incubated the transduced T cells with isotopically labeled glucose (U-$^{13}C_6$) and compared glucose metabolite labeling to cellobiose metabolite labeling. This comparison in CG-T cells revealed a striking similarity in the distribution profile of catabolized cellobiose carbons to glucose carbons (**Fig. 2b**), demonstrating that cellobiose carbons are flowing through the standard metabolic pathways. When comparing glucose catabolism in CG- versus control T cells, the distribution profiles of glucose carbons again look nearly identical, demonstrating that transgenic expression of CDT-1 and GH1-1 did not result in any changes in the fate of catabolized glucose carbons. These results confirm that our approach allows cellobiose catabolism to replace the role of glucose in feeding metabolic pathways.

Glucose deprivation in T cells leads to profound metabolic perturbations, with reductions in the amounts of metabolites from the glycolytic, glycosylation, pentose phosphate, and tricarboxylic acid (TCA) pathways, and the accumulation of low-energy and oxidative intermediates including NAD+, AMP, and oxidized glutathione (GSSG) (**Fig. S2**). To assess whether CG-T cells can use cellobiose to normalize metabolite abundances during glucose withdrawal, we compared the abundance of metabolites during incubation with cellobiose to the abundances during incubation with glucose. CG-T cells incubated with cellobiose showed rescue of core glycolytic metabolites (glucose, F16BP, and acetyl-CoA), intermediates derived from glycolysis that contribute to protein glycosylation (UDP-glucose, GlcNAc-6P, and UDP-GlcNAc), and precursors of purine and pyrimidine synthesis (ribose-5-phosphate, phosphoribosyl pyrophosphate, and inosine monophosphate) (**Fig. 2c**). Furthermore, incubation with cellobiose normalized levels of metabolites central to mitochondrial function, with increased amounts of TCA substrates (acetyl-CoA, citrate, aconitate, and α-ketoglutarate) and the accumulation of a reduced chemical environment (NADH, ATP, and GSH) (**Fig. 2c**). These results demonstrate that in CG-T cells, cellobiose is catabolized into glucose, which then replenishes several of the major metabolic pathways that are depleted during glucose deprivation.

To compare the glycolytic output of CG-T cells using cellobiose versus glucose as fuel sources, we conducted sugar stress tests using the Seahorse platform, wherein the starting condition entailed complete glucose deprivation and then the first injection was either glucose or cellobiose. CG-T cells exposed to cellobiose led to robust engagement of glycolysis, demonstrated by a ~2-fold increase in extracellular acidification rate (ECAR). Control T cells did not change ECAR when exposed to cellobiose. As expected, glucose exposure equivalently increased ECAR in both control T cells and CG-T cells (**Fig. 2d**), again demonstrating that the transgenes do not alter the capacity to engage glycolysis. These results confirm the ability to use cellobiose as a fuel source. The discrepancy between ECAR increase seen when CG-T cells were exposed to glucose versus cellobiose may be impacted by the mechanism of CDT-1 transport, namely that a proton is transported into the cell along with cellobiose (**Fig. 1a**). As catabolism of cellobiose generates protons that are excreted into the media, CDT-1 transport of cellobiose removes protons from the media, ultimately diminishing the net readout of extracellular acidification. Together, these findings demonstrate that the profound metabolic disturbances experienced by T cells upon glucose withdrawal can be ameliorated by cellobiose through the expression of CDT-1 and GH1-1.

Effector Function of Transgenic T cells is Fueled by Cellobiose During Glucose Withdrawal

Activated T cells are critically dependent on glucose for optimal anti-tumor activity, as reductions in glucose negatively impact survival, proliferation, and cytokine production. To validate whether

cellobiose could rescue these functions in transgenic T cells during glucose deprivation, we next performed a series of in vitro tests.

To assess whether cellobiose could enhance T-cell survival during glucose withdrawal, we incubated T cells ± glucose ± cellobiose for 48 h. Under light microscopy, control T cells incubated with glucose appeared large, polarized, and healthy. In contrast, glucose-deprived cells adopted the distinct morphological characteristics of dead and dying cells – that is they appeared small, shriveled, and/or blebby (**Fig. 3a**). The presence of cellobiose had no discernible effect on morphology in control cells. CG-T cells incubated with and without glucose appeared the same as their control counterparts but the inclusion of cellobiose during glucose withdrawal rescued vitality and cellular morphology akin to cells incubated with glucose. Thus, cellobiose can extend survival in CG-T cells during glucose withdrawal. We further assessed the same cell populations and their morphological characteristics by flow cytometry. When incubated with glucose, a high fraction of the control cells was large and had low granularity (FSC^{hi}, SSC^{lo}) (**Fig. 3b**). The absence of glucose shifted the cell population towards a FSC^{lo}, SSC^{hi} phenotype, commonly interpreted as dead and dying compared to their large, low granularity counterparts. Again, the presence of cellobiose made little difference for control cells. In contrast, CG-T cells incubated with cellobiose during glucose withdrawal shared the morphology of cells incubated with glucose, demonstrating that transgenic CG-T cells sustained their viability when using cellobiose as a metabolic substrate.

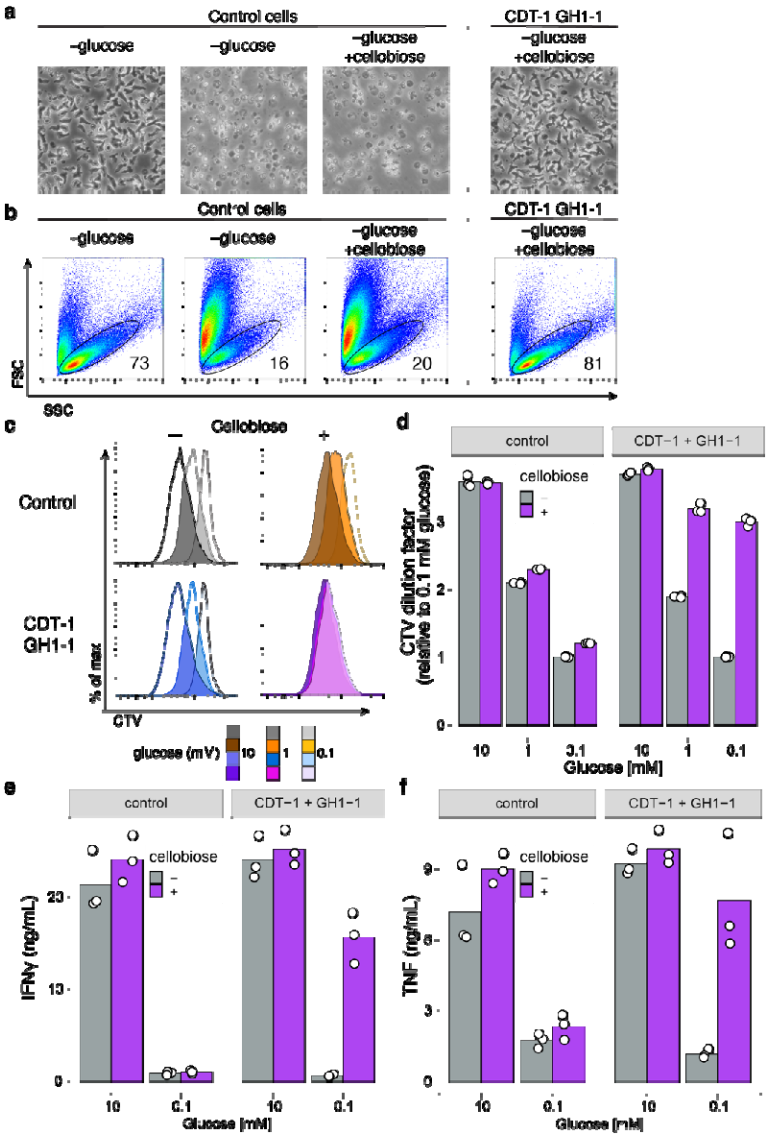

Fig. 3. Cellobiose rescues effector functions in transgenic T cells. a) Light microscopy (4x objective) of transduced T cells after 48 hours in the indicated metabolic conditions. **b**) Flow cytometry was used to assess size (FSC) and granularity (SSC) of the same cell populations as imaged in (a). **c**) Transduced T cells were stained with CTV and immediately incubated in the indicated metabolic conditions for 48 hours, before measuring the extent of CTV signal dilution. Note that the using CTV to stain and analyze activated, cycling T cells does not produce discrete, halved signal peaks from each cell division (as is typically seen when this reagent is used in the context of naïve T cell activation). **d**) Quantification of the CTV signal dilution factor from (**c**). The CTV signal dilution factor was calculated using the geometric mean of the CTV signal from each population. **e, f**) Transduced T cells were incubated in the indicated metabolic conditions for 18 h before stimulation with PMA/ionomycin for an additional 4 h. The supernatants were then collected for measurement of cytokines. Data shown in **d-f** are from technical replicates (n=3) of one experiment and are representative of at least two independent experiments.

To determine whether cellobiose could not only extend survival but also support the more resource and energy intensive process of cell division, transduced T cells were labeled with the cell proliferation dye CellTrace Violet (CTV). After CTV staining, the cells were incubated for 48 h in high to low concentrations of glucose and cellobiose was added or omitted at each concentration. We assessed proliferation by the dilution of CTV as measured by flow cytometry. As expected, reducing glucose concentration resulted in less dilution of the CTV signal (i.e., less cell proliferation) in control and CG-T cells, but the inclusion of cellobiose allowed only CG-T cells to proliferate robustly, even at the lowest glucose condition tested that otherwise eliminates proliferation (**Fig. 3c**). The proliferation of CG-T cells with cellobiose was comparable to their division seen at the highest concentration of glucose (**Fig. 3d**). Thus, cellobiose robustly supports T cell proliferation in low glucose contexts.

To measure the extent to which cellobiose can fuel cytokine production during glucose withdrawal, CG-T cells were incubated in high or low glucose ± cellobiose overnight and then restimulated with PMA/ionomycin. Glucose withdrawal profoundly reduced the production of IFN-γ and TNF, an effect seen in the percent of cytokine positive cells and the concentration of the cytokines in the supernatant (**Fig. 3e,f**; **Fig. S3**). During glucose withdrawal, CG-T cells that were incubated with cellobiose restored IFN-γ and TNF production. Thus, cellobiose fuels cytokine production in low glucose contexts.

Taken together, we show that two major effector functions of T cells—proliferation and cytokine production—are rescued by cellobiose when glucose is critically low in T cells transduced with CDT-1 and GH1-1.

In vivo proof of concept

Many diverse metabolic perturbations develop in cancer cells, affecting the extent to which glucose is depleted from their TME. As a proof of concept for our approach, we sought a suitable model system of cancer in mice that conferred a low glucose microenvironment where cellobiose-metabolizing T cells could potentially thrive in the presence of cellobiose. We subcutaneously implanted into separate mice three different syngeneic cancer cell lines (EL4-OVA (lymphoma), B16-ND4 knockout (melanoma), and MC38-OVA (adenocarcinoma)). We compared the concentration of glucose in healthy tissues (spleen, peritoneum, and skin) to the concentration in these solid tumors by LC-MS. We found that EL4-OVA and B16-ND4 KO tumors consistently had significantly reduced concentrations of glucose compared to the healthy, adjacent tissues, and that EL4-OVA tumors were more depleted of glucose than all the healthy reference tissues (**Fig. S4a**). All three types of tumors had samples with lower glucose concentrations than the healthy tissue, while MC38-OVA tumors were most heterogenous, with some tumors harboring low glucose levels and other tumors in the range of healthy tissue. Based on these results, we proceeded with the EL4-OVA model.

To determine the extent, if any, that the tumor cells themselves could benefit from the presence of cellobiose as a metabolic substrate, we incubated EL4-OVA cells in media lacking glucose but containing cellobiose and assessed the capacity to survive and divide. EL4-OVA cells were incapable of using cellobiose to facilitate proliferation (**Fig. S4b**). Furthermore, live/dead staining showed no survival advantage when cellobiose was provided in the absence of glucose (**Fig. S4c**). These results confirm that cellobiose would exclusively be available to CG-T cells as a fuel source.

For cellobiose to be available as a fuel source for adoptively transferred T cells, it must be present in the blood in high concentrations. Providing cellobiose in food or water is not a viable means of increasing blood concentration of cellobiose, due to the low rates of para- and transcellular transport of cellobiose across the intestinal epithelium, in addition to the capacity for gut microbiota to metabolize cellobiose. Instead, we opted to deliver cellobiose through repeated intraperitoneal injections. To determine the appropriate dosing schedule of cellobiose, we monitored the concentration of cellobiose in the blood after i.p. injection by LC-MS. We found that after i.p. injection, the concentration of cellobiose went up sharply into the millimolar range and returned back down to baseline within 8 h (**Fig. S4d**). Based on these results we decided to administer multiple cellobiose injections each day after the adoptive transfer of CG-T cells.

Finally, we tested the ability of CG-T cells fed with cellobiose to improve tumor clearance in a proof-of-concept experiment (**Fig. 4a**). To provide for antigen-specific targeting of T cells to the tumor, we employed OT-I TCR transgenic T cells that recognize the ovalbumin antigen expressed by EL4-OVA tumors. We implanted EL4-OVA tumors subcutaneously on day 0. We activated OT-I T cells and transduced the CDT-1 and GH1-1 transgenes as above. T cells were injected i.v. on mice on day 10. Starting on the day of T cell adoptive transfer, we delivered either cellobiose or phosphate buffered saline (PBS, control) by twice daily i.p. injections in a blinded fashion. We measured the size of the tumors by calipers and assessed for survival as determined by a tumor-size cutoff (see Methods) (**Fig. 4b**). Survival was significantly improved in the mice receiving cellobiose injections (Cox regression, $p = 0.029$) (**Fig. 4c**). The probability of survival at 30 days was 0.67 for mice treated with cellobiose and 0.25 for PBS. After the transfer of T cells, the median survival was 31 days for mice treated with cellobiose and 16 days for PBS. The hazard ratio for survival was 2.95 (95% CI 1.1 to 7.8). At 4 weeks, progression-free survival (PFS) was five of 12 (42%) for mice receiving cellobiose and 8% for control-treated mice. Two of 12 (17%) mice receiving cellobiose showed a complete response whereas none of the PBS-treated mice survived long-term. These results show that tumor growth is more heavily suppressed and survival is prolonged in mice when treated with antigen-specific T cells capable of metabolizing cellobiose.

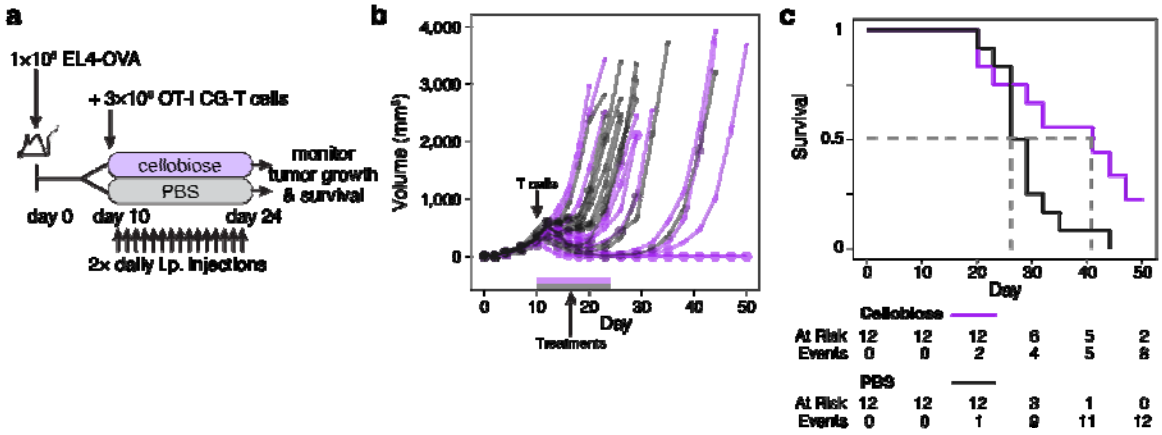

Fig. 4. **T cells that can metabolize cellobiose are a more effective treatment for cancer. a**) Schematic for the cancer experiments. **b**) Tumor volumes for mice receiving T cells on day 10 and twice daily i.p. injections of cellobiose (n=12) or PBS (n=12). Survival was defined by tumors reaching a size cutoff (see Methods). **c**) Survival curves show median survival after transfer with T cells of 31 days for mice treated with cellobiose and 16 days for mice treated with PBS. Two of twelve

mice treated with cellobiose showed a complete response. This experiment is representative of two.

Discussion

Engineered T cells (e.g., CAR-T) already play a major clinical role in fighting lymphomas. In contrast, engineered T cells have struggled to make clinical headway against solid tumors. In the solid TME, TILs (including endogenous and engineered T cells) may be directed to the correct targets but are outcompeted by the tumors for a limited supply of glucose, resulting in a stunted anti-tumor response. The upregulation of glucose transporters such as GLUT1/4 and the kinase HK2 in solid tumors result in the voracious uptake of glucose, sequestering this important nutrient away from the extracellular space[20]. Diminishment of glucose at the tissue scale in tumors can exceed ten-fold compared to healthy, adjacent tissues[21], as our own results substantiated. The impact on the immune response is profound: GLUT1 expression in human tumors negatively correlates with CD8+ T cell infiltration[22]. By engineering the ability to metabolize the natural glucose disaccharide cellobiose into antigen-specific T cells, we present a complementary approach that offers the potential to augment cancer immunotherapies like CAR-T cells in their fight against solid tumors.

There are multiple mechanisms by which provision of glucose enhances T cell responses. Glycolysis fuels the biosynthesis of nucleic acids, lipids, and amino acids. These anabolic processes are critical for cellular maintenance, cytokine production, and proliferation. We showed that carbons derived from cellobiose in our engineered T cells precisely fill those biosynthetic pathways in the absence of other sources of glucose. Deprivation of glucose inhibits expression of IFNγ in effector T cells through regulation at the epigenetic, transcriptional, and translational levels. For example, high concentrations of acetyl-CoA (which can be formed from pyruvate, a product of glycolysis) increase histone acetylation, promoting transcription of proinflammatory genes like *Ifng* and *Tnf* [5]. Additionally, certain glycolytic metabolites, like glyceraldehyde-3-phosphate, can indirectly modulate T-cell function by sequestering GAPDH away from the 3'UTR of the *Ifng* gene. This diversion releases suppressive post-transcriptional control over translation[6]. These effects are important for anti-tumor immunity, and our results confirmed that production of IFNγ in engineered T cells is rejuvenated by cellobiose in glucose-restricted conditions.

The capacity to metabolize cellobiose has potential for diverse applications. Engineering microbial cells to break down cellobiose has been explored in industrial contexts[17], and can be used for the selection of stably transduced cell lines[23]. The ability to use cellobiose as a glycolytic fuel coupled with isotopically labeled cellobiose is also a powerful tool that researchers can use to tease apart the metabolic dynamics between cells in mixed populations. For example, if tumor cells were enabled to metabolize cellobiose and co-cultured with T cells in the presence of isotopically labeled cellobiose, it might be possible to explore which cellobiose-derived (and by virtue glucose-derived) metabolites the tumor cells were producing that accumulate in and affect T cells (S. Kaech, personal communication). Another application of this work could offer cellobiose to not only enhance but also regulate the vigor of CAR-T cell responses. Many CAR-T cell responses in lymphomas are overactive in the first week and result in morbidity and mortality due to cytokine-release syndrome. If CAR-T cells fueled by cellobiose were to become overactive, the cellobiose infusions could be reduced to curtail cytokine production. Beyond cancer immunology, we believe this approach could be used to answer questions about the regulation of glucose metabolism across many cell types, biological processes, and diseases.

References and Notes

1. Bantug, G.R., Galluzzi, L., Kroemer, G., and Hess, C. (2017). The spectrum of T cell metabolism in health and disease. Nature Reviews Immunology *18*, 19–34. 10.1038/nri.2017.99.

2. Geltink, R.I.K., Kyle, R.L., and Pearce, E.L. (2018). Unraveling the Complex Interplay between T Cell Metabolism and Function. Annual Review of Immunology *36*, 461–488. 10.1146/annurev-immunol-042617-053019.

3. Ma, E.H., Verway, M.J., Johnson, R.M., Roy, D.G., Steadman, M., Hayes, S., Williams, K.S., Sheldon, R.D., Samborska, B., Kosinski, P.A., et al. (2019). Metabolic Profiling Using Stable Isotope

Tracing Reveals Distinct Patterns of Glucose Utilization by Physiologically Activated CD8+ T Cells. Immunity *51*, 856-870.e5. 10.1016/j.immuni.2019.09.003.

4. Palmer, C.S., Ostrowski, M., Balderson, B., Christian, N., and Crowe, S.M. (2015). Glucose Metabolism Regulates T Cell Activation, Differentiation, and Functions. Frontiers in Immunology *6*.

5. Peng, M., Yin, N., Chhangawala, S., Xu, K., Leslie, C.S., and Li, M.O. (2016). Aerobic glycolysis promotes T helper 1 cell differentiation through an epigenetic mechanism. Science *1002967*, aaf6284. 10.1126/science.aaf6284.

6. Chang, C.-H., Curtis, J.D., Maggi, L.B., Faubert, B., Villarino, A.V., O'Sullivan, D., Huang, S.C.-C., van der Windt, G.J.W., Blagih, J., Qiu, J., et al. (2013). Posttranscriptional Control of T Cell Effector Function by Aerobic Glycolysis. Cell *153*, 1239–1251. 10.1016/J.CELL.2013.05.016.

7. Rolf, J., Zarrouk, M., Finlay, D.K., Foretz, M., Viollet, B., and Cantrell, D.A. (2013). AMPKα1: A glucose sensor that controls CD8 T-cell memory. European Journal of Immunology *43*, 889–896. 10.1002/eji.201243008.

8. Chang, C.H., Qiu, J., O'Sullivan, D., Buck, M.D., Noguchi, T., Curtis, J.D., Chen, Q., Gindin, M., Gubin, M.M., Van Der Windt, G.J.W., et al. (2015). Metabolic Competition in the Tumor Microenvironment Is a Driver of Cancer Progression. Cell *162*, 1229–1241. 10.1016/j.cell.2015.08.016.

9. Ho, P.C., Bihuniak, J.D., MacIntyre, A.N., Staron, M., Liu, X., Amezquita, R., Tsui, Y.C., Cui, G., Micevic, G., Perales, J.C., et al. (2015). Phosphoenolpyruvate Is a Metabolic Checkpoint of Anti-tumor T Cell Responses. Cell *162*, 1217–1228. 10.1016/j.cell.2015.08.012.

10. Cham, C.M., Driessens, G., O'Keefe, J.P., and Gajewski, T.F. (2008). Glucose deprivation inhibits multiple key gene expression events and effector functions in CD8+ T cells. European Journal of Immunology *38*, 2438–2450. 10.1002/eji.200838289.

11. Blagih, J., Coulombe, F., Vincent, E.E., Dupuy, F., Galicia-Vázquez, G., Yurchenko, E., Raissi, T.C., van der Windt, G.J.W., Viollet, B., Pearce, E.L., et al. (2015). The energy sensor AMPK regulates T cell metabolic adaptation and effector responses in vivo. Immunity *42*, 41–54. 10.1016/j.immuni.2014.12.030.

12. Menk, A.V., Scharping, N.E., Moreci, R.S., Zeng, X., Guy, C., Salvatore, S., Bae, H., Xie, J., Young, H.A., Wendell, S.G., et al. (2018). Early TCR Signaling Induces Rapid Aerobic Glycolysis Enabling Distinct Acute T Cell Effector Functions. Cell Reports *22*, 1509–1521. 10.1016/j.celrep.2018.01.040.

13. Andersen, D.W., Daabees, T.T., Applebaum, A.E., Filer, L.J., and Stegink, L.D. (1983). Utilization of intravenously administered β-cellobiose and maltose by young pigs. Journal of Nutrition *113*, 1039–1045. 10.1093/jn/113.5.1039.

14. Nakamura, S., Oku, T., and Ichinose, M. (2004). Bioavailability of cellobiose by tolerance test and breath hydrogen excretion in humans. Nutrition *20*, 979–983. 10.1016/j.nut.2004.08.005.

15. Lambertz, C., Garvey, M., Klinger, J., Heesel, D., Klose, H., Fischer, R., and Commandeur, U. (2014). Challenges and advances in the heterologous expression of cellulolytic enzymes: A review. Biotechnology for Biofuels *7*, 135. 10.1186/s13068-014-0135-5.

16. Bischof, R.H., Ramoni, J., and Seiboth, B. (2016). Cellulases and beyond: The first 70 years of the enzyme producer Trichoderma reesei. Microbial Cell Factories *15*. 10.1186/s12934-016-0507-6.

17. Galazka, J.M., Tian, C., Beeson, W.T., Martinez, B., Glass, N.L., and Cate, J.H.D. (2010). Cellodextrin transport in yeast for improved biofuel production. Science *330*, 84–86. 10.1126/science.1192838.

18. Ha, S.J., Galazka, J.M., Joong Oh, E., Kordić, V., Kim, H., Jin, Y.S., and Cate, J.H.D. (2013). Energetic benefits and rapid cellobiose fermentation by Saccharomyces cerevisiae expressing

cellobiose phosphorylase and mutant cellodextrin transporters. Metabolic Engineering *15*, 134–143. 10.1016/j.ymben.2012.11.005.

19. Jang, S., Nelson, J.C., Bend, E.G., Rodríguez-Laureano, L., Tueros, F.G., Cartagenova, L., Underwood, K., Jorgensen, E.M., and Colón-Ramos, D.A. (2016). Glycolytic enzymes localize to synapses under energy stress to support synaptic function. Neuron *90*, 278–291. 10.1016/j.neuron.2016.03.011.

20. García-Canaveras, J.C., Chen, L., and Rabinowitz, J.D. (2019). The tumor metabolic microenvironment: Lessons from lactate. Cancer Research *79*, 3155–3162. 10.1158/0008-5472.CAN-18-3726.

21. Hirayama, A., Kami, K., Sugimoto, M., Sugawara, M., Toki, N., Onozuka, H., Kinoshita, T., Saito, N., Ochiai, A., Tomita, M., et al. (2009). Quantitative metabolome profiling of colon and stomach cancer microenvironment by capillary electrophoresis time-of-flight mass spectrometry. Cancer Research *69*, 4918–4925. 10.1158/0008-5472.CAN-08-4806.

22. Singer, K., Kastenberger, M., Gottfried, E., Hammerschmied, C.G., Büttner, M., Aigner, M., Seliger, B., Walter, B., Schlösser, H., Hartmann, A., et al. (2011). Warburg phenotype in renal cell carcinoma: High expression of glucose-transporter 1 (GLUT-1) correlates with low CD8+ T-cell infiltration in the tumor. International Journal of Cancer *128*, 2085–2095. 10.1002/ijc.25543.

23. Teixeira, A.P., Stücheli, P., Ausländer, S., Ausländer, D., Schönenberger, P., Hürlemann, S., and Fussenegger, M. (2022). CelloSelect – A synthetic cellobiose metabolic pathway for selection of stable transgenic CHO cell lines. Metabolic Engineering *70*, 23–30. 10.1016/j.ymben.2022.01.001.

Acknowledgments

We thank Dr. Erika Pearce for her gift of the EL4-OVA cell line. We thank Dr. Greg Delgoffe for advice and for his gift of the B16-ND4 KO cell line. We thank Michael Trump and Humza Khan for assistance with pilot experiments, and other members of the Butte lab for support. We thank Johanna ten Hoeve for her assistance with LC-MS through the UCLA Metabolomics Core. We appreciate the services of LumiGenics LLC for assistance with in vivo metabolite quantification.

Funding

This project was partially funded by the E. Richard Stiehm Endowment (MJB); UCLA Jonsson Comprehensive Cancer Center Fellowship (MLM); National Institutes of Health Ruth L. Kirschstein National Research Service Award GM007185 (MLM); National Institutes of Health grant R21 AI166551 (MJB)

Author contributions:

Conceptualization: MLM, MJB
Investigation: MLM, RN, TJT
Visualization: MLM, MJB
Funding acquisition: MLM, MJB
Supervision: MJB
Project administration: MJB
Writing – original draft: MLM, MJB
Writing – review & editing: MLM, RN, TJT, MJB

Competing interests: The Regents of the University of California have applied for a patent on this work (application # PCT/US22/24298). The authors declare no other competing interests.

Data availability: All data are available in the main text or the supplementary materials.

Supplementary Materials

Materials and Methods
Figs. S1 to S4